# Cerebral microbleeds: Prevalence and relationship to amyloid burden

**Article** *in* Neurology · December 2018

DOI: 10.1212/WNL.0000000000006780

CITATIONS
12

READS
55

**20 authors**, including:

Hugo Botha
Mayo Foundation for Medical Education and Research
**75** PUBLICATIONS **565** CITATIONS
SEE PROFILE

Jeffrey L Gunter
Mayo Foundation for Medical Education and Research
**284** PUBLICATIONS **12,785** CITATIONS
SEE PROFILE

Gregory M Preboske
Mayo Foundation for Medical Education and Research
**43** PUBLICATIONS **1,493** CITATIONS
SEE PROFILE

Matthew L Senjem
Mayo Foundation for Medical Education and Research
**405** PUBLICATIONS **13,814** CITATIONS
SEE PROFILE

Published Ahead of Print on December 19, 2018 as 10.1212/WNL.0000000000006780

ARTICLE

# Cerebral microbleeds

## Prevalence and relationship to amyloid burden

Jonathan Graff-Radford, MD, Hugo Botha, MBChB, Alejandro A. Rabinstein, MD, Jeffrey L. Gunter, PhD, Scott A. Przybelski, BS, Timothy Lesnick, MS, John Huston, III., MD, Kelly D. Flemming, MD, Gregory M. Preboske, BS, Matthew L. Senjem, MS, Robert D. Brown, Jr., MD, Michelle M. Mielke, PhD, Rosebud O. Roberts, MBChB, Val J. Lowe, MD, David S. Knopman, MD, Ronald C. Petersen, MD, PhD, Walter Kremers, PhD, Prashanthi Vemuri, PhD, Clifford R. Jack, Jr., MD, and Kejal Kantarci, MD

**Correspondence**
Dr. Graff-Radford
Graff-Radford.Jonathan@mayo.edu

*Neurology*® 2019;92:e1-e10. doi:10.1212/WNL.0000000000006780

## Abstract

### Objective

To describe the prevalence of cerebral microbleeds (CMBs) and determine the association between CMBs and β-amyloid burden on PET.

### Methods

From the population-based Mayo Clinic Study of Aging, 1,215 participants (53% male) underwent 3-tesla MRI scans with T2* gradient recalled echo sequences from October 2011 to February 2017. A total of 1,123 participants (92%) underwent $^{11}$C-Pittsburgh compound B (PiB)-PET scans. The prevalence of CMBs was derived by adjusting for nonparticipation and standardizing to the Olmsted County, MN, population. The relationship between β-amyloid burden and CMB presence and location was tested using logistic regression models. Ordinal logistic models tested the relationship between CMB frequency and β-amyloid burden.

### Results

Two hundred seventy-four participants (22.6%) had at least one CMB. CMB frequency increased with age by decade (11% aged 60–69 years, 22% 70–79 years, and 39% 80 years and older). After adjusting for age, sex, and hypertension, PiB standardized uptake value ratio (SUVR) was associated with increased odds of a CMB. The association between PiB SUVR and CMBs was location-specific; PiB SUVR was associated with lobar CMBs but not deep CMBs. Age, hypertension, and PiB SUVR were associated with increasing CMB count. CMB density was greatest in parietal and occipital regions; β-amyloid burden correlated with concentration of CMBs in all lobar regions. Among participants with multiple CMBs, greater PiB uptake occurred in the pre- and postcentral gyri superiorly, the superior parietal lobe and precuneus, the angular gyrus, inferior temporal gyrus, and temporal poles.

### Conclusions

The prevalence of CMBs increases with age. In this population-based sample, β-amyloid load was associated with lobar but not with deep CMBs.

RELATED ARTICLE

Are lobar microbleeds of diagnostic value in the community?
Page 121

From the Departments of Neurology (J.G.-R., H.B., A.A.R., K.D.F., R.D.B., M.M.M., R.O.R., D.S.K., R.C.P.), Radiology (J.L.G., J.H., G.M.P., M.L.S., V.J.L., P.V., C.R.J., K.K.), and Health Sciences Research (S.A.P., T.L., M.M.M., R.O.R., W.K.), Mayo Clinic, Rochester, MN.

Go to Neurology.org/N for full disclosures. Funding information and disclosures deemed relevant by the authors, if any, are provided at the end of the article.

## Glossary

**AD** = Alzheimer disease; **ANTs** = Advanced Normalization Tools; **ARIA-H** = amyloid-related imaging abnormalities–hemosiderin; **CAA** = cerebral amyloid angiopathy; **CMB** = cerebral microbleed; **GRE** = gradient recalled echo; **MCALT** = Mayo Clinic Adult Lifespan Template; **MCSA** = Mayo Clinic Study of Aging; **PiB** = Pittsburgh compound B; **SUVR** = standardized uptake value ratio.

Cerebral microbleeds (CMBs), detected on hemosiderin-sensitive MRI sequences, are a common cerebrovascular pathology in the aging population and a known risk for intracerebral hemorrhage and ischemic stroke.[1,2] CMB location may predict the primary pathology: lobar CMBs correlate with cerebral amyloid angiopathy (CAA) and deep CMBs with hypertensive arteriopathy.[3,4]

Prior studies have used amyloid PET to study CMB pathogenesis in individuals with CAA, Alzheimer disease (AD), and vascular dementia. β-Amyloid burden was associated with lobar CMBs while deep CMBs correlated with MRI findings of hypertensive small vessel disease.[4,5] Population- and community-based studies have shown an association with the *APOE* ε4 allele or atrophy in AD signature regions suggesting CAA as a possible cause of lobar CMBs.[6–8] Previous studies of CMBs with amyloid PET have not been population-based[4,5,9,10]; therefore, it is unclear whether CMBs in the general population are related to β-amyloid burden. This is important because CMBs may identify asymptomatic individuals at increased risk of intracerebral hemorrhage and cognitive decline. The objectives of this study were (1) to describe the prevalence of CMBs and (2) to investigate the relationship between CMBs and β-amyloid burden on PET in a population-based sample.

## Methods

### Study participants

Participants were enrolled in the Mayo Clinic Study of Aging (MCSA), a longitudinal, population-based study of cognitive decline. The MCSA study design has been published previously.[11] In the MCSA, Olmsted County residents without dementia were identified and randomly selected using the Rochester Epidemiology Project medical records linkage system and stratified by age and sex for enrollment in the study.[12] Each participant underwent an in-person evaluation including a nurse or study coordinator interview, a neurologic evaluation, and neuropsychological testing. Afterward, a diagnosis of dementia was based on consensus agreement among the examining physician, nurse, and neuropsychologist taking into account education and potential confounders such as hearing loss.[11]

Participants without contraindications were invited to undergo brain MRI and PET imaging. In October 2011, T2* gradient recalled echo (GRE) sequences were added to the neuroimaging protocol. Participants imaged with T2* GRE sequences between October 2011 and February 2017 were included in this study. We evaluated 3,077 participants during the study; 1,232 underwent an MRI scan with T2* GRE sequences. To maximize those with concurrent amyloid PET scans, the most recent MRI scan was selected for analysis. We excluded 17 scans that failed quality control. Therefore, 1,215 participants with useable T2* were included in the analysis.

### Standard protocol approvals, registrations, and patient consents

The MCSA and associated studies were approved by the Mayo Clinic and Olmsted Medical Center institutional review boards. Written informed consent was obtained from all participants before they joined the study.

### Clinical data retrieval

Clinical data, including history of diabetes, smoking, hypertension, and dyslipidemia, were abstracted by a nurse from the detailed medical records included in the medical records linkage system.[12]

### Prevalence estimates

An inverse probability weighting approach was used to convert our observed frequencies of CMBs to population prevalence. To account for the time between study entry and scan, the inverse probability was split into a 2-step process accounting for study entry (step 1) adjusting for age, sex, and education and whether imaging was performed and (step 2) additionally adjusting for prevalent cognitive impairment. This accounts for 2 potential types of bias: (1) study nonparticipation and (2) imaging nonparticipation. The details of the approach in the MCSA have been previously published.[13,14]

### MRI examination and identification of CMBs

All images were obtained using 3-tesla MRI scanners. The complete details of the acquisitions were previously published.[15] A T2* GRE was performed with the following parameters: repetition time/echo time = 200/20 milliseconds; flip angle = 12°; in-plane matrix = 256 × 224; phase field of view = 1.00; and slice thickness = 3.3 mm. Acquisition time (5 minutes) was used to grade CMBs. On the MRI, CMBs are defined according to consensus criteria[3] as homogeneous hypointense lesions in the gray or white matter, which are distinct from iron or calcium deposits and vessel flow voids on T2* GRE images.[16] All CMBs were identified by trained image analysts and secondarily confirmed by a vascular neurologist experienced in interpreting the T2* GRE images. When it was not possible to distinguish a CMB definitively from a flow void, the CMB was recorded as a "possible CMB." Possible CMBs

were excluded from analysis because of the nondefinitive nature of the finding. All scans were read by a single investigator (J.G.-R.) blinded to the participants' clinical information. The intrarater reliability based on blinded reading on 2 separate occasions was excellent (κ statistic 0.86). The interrater agreement between a neuroradiologist and neurologist (J.H., J.G.-R.) on definite vs not-definite CMB was 87%, corresponding to good agreement (κ 0.68).

## Tracking and registration of CMBs to a common template

The location of each CMB was recorded in the coordinate system of the image on which it was made. A structural T1 (MPRAGE [magnetization-prepared rapid-acquisition gradient echo]) image of the participant was registered and resampled into the GRE image. An in-house, modified, automated anatomical-labeling atlas was used to delineate bilateral frontal, parietal, temporal, and occipital lobar regions as well as deep/infratentorial gray and white matter regions.[17] CMBs were classified as lobar with or without cerebellar CMBs, and deep/infratentorial CMBs with or without cerebellar CMBs. Because lobar regions vary in volume, we compared the regional CMB density referenced to regional volume instead of counts per region.[16]

Composite maps of CMB locations across participants were built by transforming T2* GRE image locations into the space of the Mayo Clinic Adult Lifespan Template (MCALT).[18] Using image registration, we determined the affine transformation from coordinates in the T2* GRE space to T1-weighted image space. For each CMB, a distance map in T1-weighted image space was constructed. We used the Advanced Normalization Tools (ANTs) suite to perform high-dimensional warping. The ANTs methods ensure that the deformations are diffeomorphic. Using ANTs,[19] the T1-weighted image was warped to the MCALT template. The resulting transformation was applied to each distance map. The position of each CMB in MCALT space was taken from the minimum of the deformed distance map. A small sphere placed around each CMB in MCALT made it viewable on 3-dimensional rendering; overlapping spheres merged forming clusters.

## $^{11}$C-Pittsburgh compound B–PET acquisition

Amyloid PET imaging was completed with $^{11}$C-Pittsburgh compound B (PiB). PET images were acquired with a PET/CT operating in 3-dimensional mode (DRX; GE Healthcare, Waukesha, WI). The details of PET acquisition were previously published.[20,21] Attenuation-corrected PiB-PET images were processed using our in-house, fully automated pipeline.[22] This includes coregistration of each participant's structural MRI to their PiB-PET image, spatial normalization to template space, and smoothing. Regions of interest are propagated from an MRI template to be used in PiB-PET analyses. Gray and white matter sharpening was applied, during which voxels with a higher likelihood of being CSF than either gray or white matter are excluded from the region-of-interest statistics.

A global cortical PiB-PET standardized uptake value ratio (SUVR) was calculated as the voxel size-weighted median uptake in the precuneus, anterior and posterior cingulate, prefrontal, orbitofrontal, parietal, and temporal regions of interest after normalization to the uptake in the cerebellar gray matter.[23]

Voxel-wise analyses were performed in SPM 12 comparing amyloid PET uptake in those with no CMB vs those with ≥2, with age included as a covariate (fil.ion.ucl.ac.uk/spm/software/spm12). Results were viewed and corrected for multiple comparisons using correction at the cluster level. A cluster size of 192 was determined by running 5,000 Monte Carlo simulations with REST AlphaSim using an individual voxel threshold probability of 0.001.[24]

## Statistical analysis

Demographic and clinical characteristics of the participants were summarized using means and SDs for continuous variables and counts and percentages for categorical variables. The distributions of the continuous variables were examined for approximate symmetry and normality using plots; PiB SUVR was subsequently log-transformed for statistical tests to reduce a positive skew. The results in the characteristics (tables 1 and 2) were compared using *t* tests for continuous variables and $\chi^2$ tests for categorical variables. The participants were first classified in a binary fashion (CMB present/absent) by location (any CMB, lobar only, deep only) and then into 4 categorical CMB groups (0, 1, 2–4, 5+) to

**Table 1** Characteristics based on presence of CMB

| | All (n = 1,215) | None (n = 941) | CMB (n = 274) | *p* Value |
|---|---|---|---|---|
| **Male** | 648 (53) | 465 (49) | 183 (67) | <0.001 |
| **Age, y, mean (SD)** | 74.1 (8.6) | 72.8 (8.2) | 78.7 (8.3) | <0.001 |
| ***APO* ε4 allele carrier** | 337 (28) | 261 (28) | 76 (28) | 0.98 |
| **Education, y, mean (SD)** | 14.7 (2.6) | 14.7 (2.6) | 14.7 (2.7) | 0.73 |
| **PiB SUVR, mean (SD)** | 1.56 (0.41) | 1.52 (0.37) | 1.68 (0.48) | <0.001[a] |
| **Diabetes** | 214 (18) | 163 (17) | 51 (19) | 0.60 |
| **Hypertension** | 795 (65) | 587 (62) | 208 (76) | <0.001 |
| **Dyslipidemia** | 999 (82) | 771 (82) | 228 (84) | 0.55 |
| **Smoker (ever)** | 565 (47) | 435 (46) | 130 (47) | 0.73 |
| **Demented** | 16 (1) | 7 (1) | 9 (3) | 0.001 |

Abbreviations: CMB = cerebral microbleed; PiB = Pittsburgh compound B; SUVR = standardized uptake value ratio.
The mean (SD) are listed for the continuous variables and count (%) for the categorical variables. The *p* values between groups (none and CMB) are from a *t* test for continuous variables or a $\chi^2$ test for the categorical variables.
[a] Because of skewness, the statistical test was done on the log transformation of the variable.

**Table 2** Number of CMBs based on age strata

| | All (n = 1,215) | 60–69 y (n = 485) | 70–79 y (n = 390) | 80+ y (n = 340) | *p* Value |
|---|---|---|---|---|---|
| **No CMB** | 941 (912, 970), 77 | 430 (416, 444), 89 | 305 (289, 321), 78 | 206 (188, 224), 60 | <0.001 |
| **1 CMB** | 158 (135, 181), 13 | 40 (28, 52), 8 | 48 (35, 61), 12 | 70 (55, 85), 21 | |
| **2–4 CMBs** | 85 (68, 102), 7 | 11 (5, 17), 2 | 27 (17, 37), 7 | 47 (35, 59), 14 | |
| **5+ CMBs** | 31 (20, 42), 3 | 4 (0, 8), 1 | 10 (4, 16), 3 | 17 (9, 25), 5 | |

Abbreviation: CMB = cerebral microbleed.
The counts (95% confidence intervals), frequencies are listed for CMBs. The *p* values between groups are a $\chi^2$ test.

determine an association between increasing frequency of CMBs and β-amyloid burden. Logistic models were used to test the relationship between CMBs and β-amyloid burden by location (table 3). Table 3 includes only participants who had both a GRE scan and an amyloid PET scan. Ordinal logistic models were used to test the relationship between increasing CMBs and β-amyloid burden (table 4). Because of the low frequency of individuals with multiple deep CMBs, the ordinal regression model was not stratified by location. These models also tested for associations of CMBs with age, sex, hypertension, *APOE* ε4 carrier status, diabetes, dyslipidemia, and smoking (ever/never). Backward-elimination and forward-selection procedures were used to select terms for the final parsimonious models (the 2 approaches produced the same models using $\alpha = 0.05$). All 2-way interactions were considered among the significant univariate results with only the significant results being reported. Lastly, Spearman rank correlations were calculated to investigate the strength of the association of regional CMB density and regional β-amyloid load.

### Data availability

Data from the MCSA including data from this study are available on request.

## Results

The demographics of the study cohort by CMB status are reported in table 1. Of 1,215 participants with mean (SD) age of 74.1 (8.6) years who underwent MRI T2* GRE sequences, 648 (53%) were men; 1,123 (92%) underwent PiB-PET scans. The age range of participants was 60 to 98 years. Participants with CMBs were older (mean [SD] age 78.7 [8.3] years vs 72.8 [8.2] without CMBs, $p < 0{\cdot}001$), more likely male (183 [67%] vs 465 [49%], $p < 0.001$), and more likely hypertensive (208 [76%] vs 587 [62%], $p < 0.001$). PiB SUVR was higher in those with CMBs (1.68 [0.48] vs those without CMBs 1.52 [0.37], $p < 0{\cdot}001$). While participants were dementia-free at study enrollment, at the time of T2* MRI, those with CMBs were more likely to have dementia (9 [3%] vs 7 [1%], $p = 0.001$).

The frequency of CMBs by decade is reported in table 2. CMBs increased in frequency from 11% among ages 60–69 years, to 22% among ages 70–79 years, and to 39% among those older than 80 years with an overall frequency of 23%. The presence of multiple CMBs also increased with age.

The weighted prevalence of CMBs based on the inverse propensity weighting for individuals aged 60–89 years was 18.1% overall, 11.9% among ages 60–69 years, 19.1% among ages 70–79 years, and 33.5% among those older than 80 years.

Lobar-only CMBs occurred in 199 individuals, deep/infratentorial-only in 32, mixed lobar and deep in 25 individuals, and cerebellar-only in 18. Among the 274 participants with a CMB, there was an average (mean) of 3.5 CMBs with a median of 1 CMB and range of 1 to 209.

Univariate logistic regressions with at least one CMB (any, lobar-only, deep or infratentorial-only) as the response variable showed associations between age, male sex, PiB SUVR, and hypertension with the presence of a CMB, but there was no association with *APOE* ε4 carrier status, diabetes, dyslipidemia, and smoking history (table 3). In the final model, which included significant covariates, PiB SUVR was associated with the presence of a CMB (table 3). When divided by location, there was only a significant relationship between PiB SUVR and presence of lobar-only CMBs but not deep/infratentorial CMBs. Among those with a lobar location, there was a significant interaction between PiB SUVR and hypertension such that at lower PiB SUVR having hypertension tends to increase risk of having a lobar CMB. At the higher end of PIB SUVR, hypertension is unassociated with the development of a lobar CMB. Others have characterized the deep/infratentorial group as any deep or infratentorial CMB (deep only + deep and lobar). Using any deep CMB (n = 54), rather than deep-only, did not change the results. CMBs were associated with age (1.32 [1.11, 1.57], $p = 0.002$) but not PiB SUVR (1.04 [0.92, 1.17], $p = 0.57$).

Univariate ordinal logistic regressions with increasing CMB frequency (0, 1, 2–4, 5+ CMBs) as the response variable showed associations between age, male sex, PiB SUVR, and hypertension with a higher number of CMBs, but there was no association with *APOE* ε4 carrier status, diabetes, dyslipidemia, and smoking history (table 4). In the final model, which included significant covariates, PiB SUVR was associated with increasing CMB burden, with odds ratio (95% confidence

**Table 3** Factors associated with any, lobar-only, and deep/infratentorial-only CMBs

| | Any CMB (deep, lobar, or both) (n = 274) | | | | Lobar-only (n = 199) | | | | Deep/infratentorial-only (n = 32) | | | |
|---|---|---|---|---|---|---|---|---|---|---|---|---|
| | Univariate models | | Final model | | Univariate models | | Final model | | Univariate models | | Final model | |
| | OR (95% CI) | *p* Value | OR (95% CI) | *p* Value | OR (95% CI) | *p* Value | OR (95% CI) | *p* Value | OR (95% CI) | *p* Value | OR (95% CI) | *p* Value |
| **Age** | 1.51 (1.38, 1.64) | <0.001 | 1.83 (1.50, 2.24) | <0.001 | 1.51 (1.38, 1.66) | <0.001 | 1.46 (1.31, 1.63) | <0.001 | 1.41 (1.15, 1.73) | 0.001 | 1.31 (1.03, 1.65) | 0.03 |
| **Male** | 2.06 (1.55, 2.73) | <0.001 | 1.82 (1.34, 2.47) | <0.001 | 2.16 (1.56, 2.98) | <0.001 | 1.78 (1.26, 2.52) | 0.001 | 0.80 (0.39, 1.62) | 0.53 | — | — |
| **PiB SUVR** | 1.18 (1.11, 1.25) | <0.001 | 2.77 (1.38, 5.54) | 0.004 | 1.17 (1.10, 1.25) | <0.001 | 1.20 (1.03, 1.39) | 0.02 | 1.17 (1.02, 1.35) | 0.03 | 1.05 (0.90, 1.23) | 0.53 |
| **Hypertension** | 1.93 (1.42, 2.63) | <0.001 | 1.31 (0.94, 1.85) | 0.12 | 1.88 (1.33, 2.68) | <0.001 | 2.57 (1.11, 5.96) | 0.03 | 2.61 (1.07, 6.41) | 0.04 | 2.31 (0.86, 6.23) | 0.10 |
| **Age × PiB**[a] | — | | 1.13 (1.05, 1.23) | 0.002 | — | — | — | — | — | — | — | — |
| **PiB × no hypertension**[a] | — | — | — | — | | | 1.20 (1.03, 1.39) | 0.02 | | | | |
| ***APO* ε4 allele carrier**[b] | 1.00 (0.74, 1.36) | 0.98 | — | — | 1.00 (0.71, 1.40) | 0.98 | | | 1.18 (0.55, 2.52) | 0.67 | | |
| **Diabetes**[b] | 1.10 (0.77, 1.55) | 0.60 | — | — | 1.13 (0.77, 1.68) | 0.53 | | | 1.10 (0.45, 2.72) | 0.83 | | |
| **Dyslipidemia**[b] | 1.12 (0.78, 1.60) | 0.55 | — | — | 1.10 (0.73, 1.66) | 0.64 | | | 2.13 (0.64, 7.08) | 0.22 | | |
| **Smoker (ever)**[b] | 1.05 (0.80, 1.37) | 0.73 | — | — | 1.10 (0.81, 1.50) | 0.53 | | | 1.02 (0.51, 2.08) | 0.95 | | |

Abbreviations: CI = confidence interval; CMB = cerebral microbleed; OR = odds ratio; PiB = Pittsburgh compound B; SUVR = standardized uptake value ratio.
Logistic model with CMB as the response where CMBs are split into 2 groups: none, 1 or more. All PiB SUVR results are based on a 0.1-unit SUVR increase on the log scale; age is based on 5-year increase.
[a] The interaction is for a 0.1-unit SUVR increase in log PiB at age 75 years.
[b] These were not included for the final model.

**Table 4** Factors associated with CMB frequency

| | Any CMB (deep, lobar, or both) (n = 274) | | | |
|---|---|---|---|---|
| | Univariate models | | Final model | |
| | OR (95% CI) | *p* Value | OR (95% CI) | *p* Value |
| **Age** | 1.52 (1.40, 1.65) | <0.001 | 1.82 (1.50, 2.22) | <0.001 |
| **Male** | 2.08 (1.57, 2.75) | <0.001 | 1.83 (1.35, 2.47) | <0.001 |
| **PiB SUVR** | 1.18 (1.12, 1.25) | <0.001 | 2.74 (1.40, 5.39) | 0.003 |
| **Hypertension** | 1.96 (1.44, 2.66) | <0.001 | 1.34 (0.95, 1.87) | 0.09 |
| **Age × PiB**[a] | — | | 1.14 (1.06, 1.23) | <0.001 |
| ***APO* ε4 allele carrier**[b] | 1.04 (0.77, 1.39) | 0.82 | — | — |
| **Diabetes**[b] | 1.14 (0.81, 1.60) | 0.46 | — | — |
| **Dyslipidemia**[b] | 1.15 (0.80, 1.64) | 0.46 | — | — |
| **Smoker (ever)**[b] | 1.03 (0.79, 1.35) | 0.81 | — | — |

Abbreviations: CI = confidence interval; CMB = cerebral microbleed; OR = odds ratio; PiB = Pittsburgh compound B; SUVR = standardized uptake value ratio. All PiB SUVR results are based on a 0.1-unit SUVR increase on the log scale; age is based on 5-year increase. Ordinal logistic model with CMB as the response where total CMBs are split into 4 groups: none, 1, 2–4, 5+.
[a] The interaction is for a 0.1-unit SUVR increase in log PiB at age 75 years.
[b] These variables were not included for the final model.

interval) (2.74 [1.40, 5.38], $p = 0.003$), though this should be interpreted accounting for a significant interaction of PiB SUVR with age (1.14 [1.06, 1.23], $p < 0.001$) (table 4). At younger ages, being amyloid-positive increased the probability risk of a CMB, and as a participant aged (80+), the risk of CMBs tended to be more closely associated with age such that the effect of amyloid positivity was mitigated with increasing age.

Table 5 displays the regional lobar CMB densities and their correlations with regional β-amyloid burden. Higher concentrations of CMBs were present in the parietal and occipital lobes followed by the temporal and frontal lobes (number/L). Regional PiB SUVR correlated with CMB density in all lobar regions, though significant, the strength of each correlation was not large.

Figure 1 depicts the distribution of individual CMBs at baseline among all participants except 2 outliers with 209 and 74 CMBs at baseline who were not included in the composite map. CMBs appeared equally distributed between hemispheres and more concentrated in parietal, occipital, and temporal lobes relative to the frontal lobe.

Figure 2 displays the topographic relationship between PiB-PET uptake and the presence of ≥2 CMBs. Participants with ≥2 CMBs had increased amyloid deposition in left pre- and postcentral gyri superiorly, the superior parietal and precuneus bilaterally, the left angular gyrus, left inferior temporal gyrus, and bilateral temporal poles (family-wise error rate 0.05, cluster-level correction of k = 192 voxels). Renders of MCALT were created using BrainNet Viewer (nitrc.org/projects/bnv/).[25]

# Discussion

In this population-based study of individuals aged 60 years and older, CMBs were common, and their prevalence increased steeply with age. CMBs had a greater density in posterior brain regions. This study expands on findings of prior population-based studies by demonstrating (1) a relationship between global amyloid burden and location of CMBs, suggesting a different underlying pathophysiology for CMBs depending on location, (2) an association between regional lobar amyloid burden and regional CMB density, and (3) an association between amyloid burden in temporal, occipital, and parietal regions with the presence of 2 or more CMBs.

The PiB-hypertension and age-PiB interactions observed in our study have important implications. Hypertension is

**Table 5** Relationship between CMB density and PiB SUVR by region

| Among all participants | | | | |
|---|---|---|---|---|
| | | | Spearman correlations[b] | |
| Location | CMB density,[a] mean (SD) | PiB SUVR,[b] mean (SD) | ρ | *p* Value |
| **Frontal** | 0.52 (5.14) | 1.68 (0.34) | 0.12 | <0.001 |
| **Occipital** | 0.62 (6.59) | 1.52 (0.22) | 0.11 | <0.001 |
| **Temporal** | 0.55 (5.25) | 1.53 (0.30) | 0.10 | <0.001 |
| **Parietal** | 0.83 (9.34) | 1.66 (0.33) | 0.13 | <0.001 |

Abbreviations: CMB = cerebral microbleed; PiB = Pittsburgh compound B; SUVR = standardized uptake value ratio.
[a] Based on 1,215 participants (224 with 1+ lobar bleed).
[b] Based on 1,123 participants.

**Figure 1** Distribution of individual cerebral microbleeds at baseline

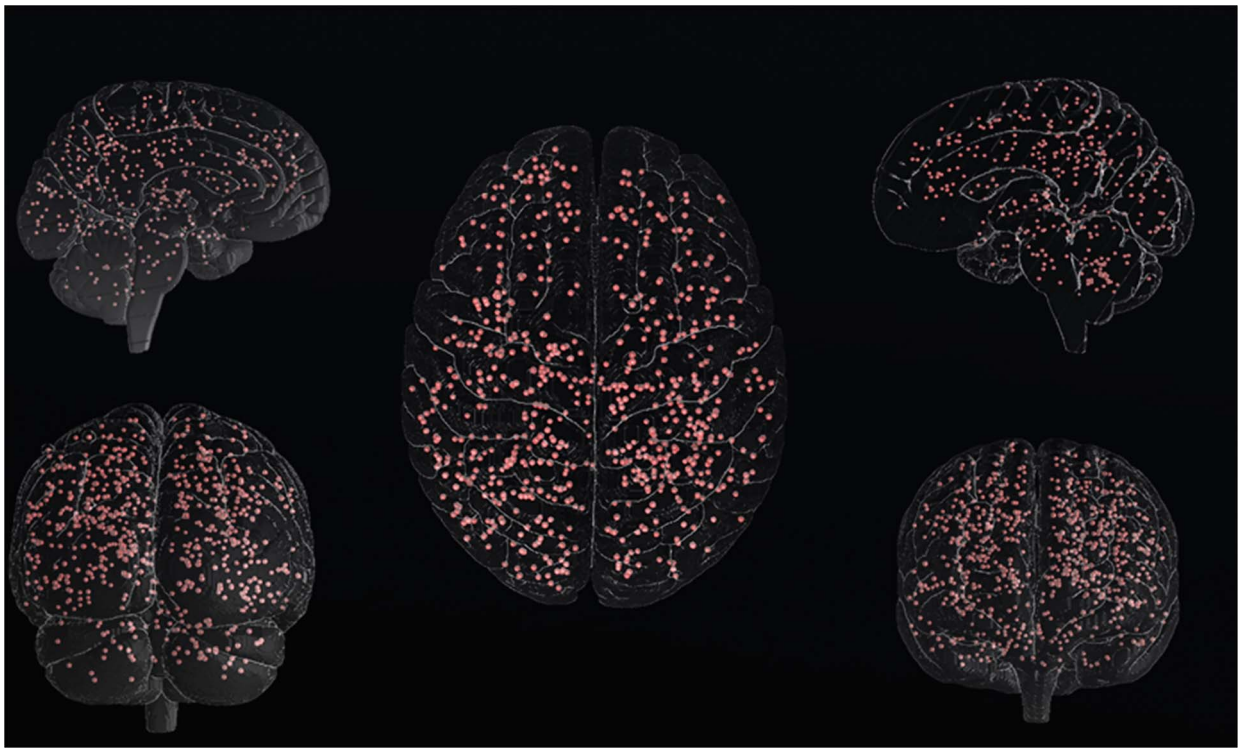

associated with lobar CMBs among amyloid-negative individuals, likely reflecting the subset of lobar CMBs due to hypertension rather than amyloid angiopathy. The stronger association between amyloid burden and CMBs at younger age reflects the fact that being amyloid-positive at younger ages increases the risk of a CMB, but this risk decreased with age possibly as multiple risk factors for CMBs, including hypertension, accumulate.

The frequency of CMBs in the MCSA was similar to the population-based Rotterdam study, but the Rotterdam study did not acquire information on amyloid deposition.[1,6] Prior population-based studies have demonstrated a similar increase in CMBs with age,[1,7] approaching 40% in those 80 years and older. The increased burden of CMBs with age and the association with amyloid load is clinically important. Approximately 37% of patients with atrial fibrillation are also 80 years and older.[26] Therefore, as the population ages, an increasing number of older patients will have greater risk of ischemic stroke from atrial fibrillation—thus having an indication for anticoagulation—while also having CMBs with a possible high amyloid burden. CMBs are a strong risk factor for hemorrhagic stroke,[2] which leads to clinical management dilemmas: is it safe to perform anticoagulation in older patients with multiple lobar CMBs? If anticoagulation might not be safe in these increasingly common patients, is MRI necessary for risk stratification?[27] This study improves our knowledge regarding the pathogenesis of CMBs by demonstrating their relationship with amyloid burden in a population-based sample. Whether additional knowledge of amyloid burden can improve intracerebral hemorrhage risk prediction in the general population will be an important area of future research.

The relationship between CMBs and *APOE* ε4 carrier status is complex. In the Rotterdam and Framingham studies, *APOE* ε4 carriers were more likely to have lobar-only CMBs.[6,7] In the Atherosclerosis Risk in Communities study, only *APOE* ε4 homozygotes had an increased probability of lobar CMBs.[28] None of these previous studies investigated the influence of β-amyloid load on the relationship between *APOE* ε4 and CMBs. In the present study, *APOE* ε4 was not associated with CMBs, but amyloid burden correlated with lobar CMBs. Whether including amyloid burden in the model mitigates *APOE* ε4 in the other studies is unknown. The relationship between *APOE* ε4 and CMBs might be stronger among participants with Alzheimer dementia when CMBs are more common.[16]

Amyloid burden correlated with the presence of CMBs. When categorized by location, amyloid load correlated with lobar CMBs but not deep/infratentorial CMBs. This parallels findings in patients with Alzheimer dementia or vascular cognitive impairment, in whom amyloid burden has also been associated with lobar-only CMBs.[4] Thus, our observations support the concept that lobar CMBs are often caused by CAA, even in the general population, but hypertension remains a cause in the absence of amyloid. This finding has relevance for patients with AD and AD clinical trials. Patients

**Figure 2** Three-dimensional brain renderings showing results of PiB-PET analysis in participants with multiple CMBs compared to those with no CMBs

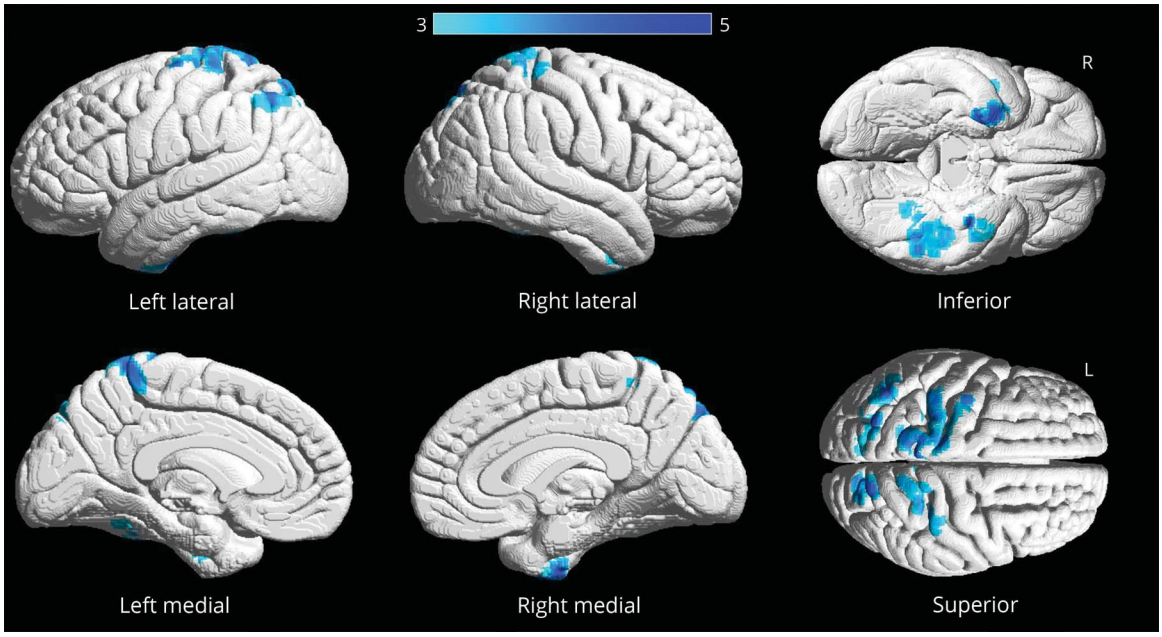


Participants with multiple CMBs (≥2) had greater PiB-PET uptake in the left pre- and postcentral gyri superiorly, the superior parietal and precuneus bilaterally, the left angular gyrus, left inferior temporal gyrus, and bilateral temporal poles. Results shown after family-wise error correction at the cluster level, with higher *t* values shown in darker blue. Renders created using Brain Net Viewer (Xia et al.)[25] (nitrc.org/projects/bnv/). CMB = cerebral microbleed; PiB = Pittsburgh compound B.

with AD who have CMBs have increased risk of stroke and cardiovascular mortality.[29] Meanwhile, CMBs are a recently recognized adverse event in AD clinical trials. A subset of research participants receiving antiamyloid therapies for AD develop new CMBs as a complication of treatment, termed amyloid-related imaging abnormalities–hemosiderin (ARIA-H).[30] ARIA-H correlates with the presence of the *APOE* ε4 allele (particularly in ε4 homozygotes) and amyloid deposition.[31] Understanding relationships of CMBs, *APOE* status, and amyloid load in persons without dementia may better inform predictions of who might develop ARIA-H in a clinical trial setting as trials now expand to treat cognitively normal individuals with elevated amyloid burden.[32]

Deep CMBs are thought to be related to hypertensive damage of deep penetrating arteries.[3] Supporting this relationship, in the Rotterdam study,[6] hypertension, increased white matter hyperintensity burden, and lacunar infarcts were associated with deep CMBs. In the current study, lobar CMBs were more common than deep CMBs. Longitudinal studies will provide additional information on the specific risk factors that increase the risk of deep CMBs.

Studying the pathology of CMBs in the community setting is difficult because the number of participants with multiple CMBs undergoing autopsy is limited. Furthermore, since CAA is a patchy disease, sampled regions may be remote from the CMBs. Among a small group of autopsied Framingham participants with ≥2 lobar CMBs, only one had moderate to severe CAA at autopsy.[33] Our finding that hypertension was associated with lobar CMBs among those who were amyloid negative supports the findings that CMBs in the general population come from multiple underlying causes including hypertension. Amyloid PET may help distinguish underlying mechanisms.

Similar to CMB distribution in patients with AD,[16] CMB concentrations were greater in parietal, occipital, and temporal lobes than in frontal lobes. A topographic relationship existed between regional PiB SUVR and regional CMB density in all lobar regions consistent with CAA underlying a subset of lobar CMBs. Amyloid burden in the temporal, parietal, and occipital regions was associated with 2 or more CMBs. These regions have a high rate of CAA at autopsy.[34] Intracerebral hemorrhage due to CAA preferentially occurs in the temporal and occipital lobes.[35] Prior studies have shown a relationship between regional amyloid load and future CMB location.[10] Longitudinal population-based studies will also be able to address the risk of future intracerebral hemorrhage in the presence of CMBs and whether CMB burden or amyloid load can identify those at highest risk.

Strengths of this study include the large population-based sample size and our ability to convert our observed frequencies of CMBs to population prevalence. The weighted prevalence of CMBs by age group was similar to the observed

frequencies but slightly lower except between ages 60 and 69 years. We used 3-tesla MRI to detect CMBs, and many patients underwent amyloid PET imaging. Limitations include the cross-sectional nature of the data and that susceptibility weighted imaging may be more sensitive to CMBs than the GRE. While we attempted to adjust for potential sources of bias through inverse probability weighting, using the most recent scan available may have introduced the potential bias of including older and healthier participants. Given the cross-sectional and exploratory nature of this study, we did not adjust for multiple comparisons, which could introduce the possibility of false-positive findings.

In a population-based study, the frequency of CMBs increased substantially with age. Amyloid burden correlates with increasing CMB frequency, which supports CAA as the pathologic substrate for multiple lobar CMBs even in asymptomatic persons. Identifying individuals at higher risk of intracerebral hemorrhage or complications from antiamyloid therapy will be important future directions.

## Author contributions

Jonathan Graff-Radford: conception of the study, acquisition and analysis of data, drafting significant portion of manuscript and figures. Hugo Botha: acquisition and analysis of data, drafting significant portion of manuscript and figures. Alejandro A. Rabinstein: conception of the study, acquisition and analysis of data, drafting significant portion of manuscript and figures. Jeffrey L. Gunter: acquisition and analysis of data, drafting significant portion of manuscript and figures. Scott A. Przybelski: acquisition and analysis of data, drafting significant portion of manuscript and figures. Timothy Lesnick: acquisition and analysis of data. John Huston III: conception of the study, acquisition and analysis of data, drafting significant portion of manuscript and figures. Kelly D. Flemming: conception of the study, acquisition and analysis of data, drafting significant portion of manuscript and figures. Gregory M. Preboske: acquisition and analysis of data. Matthew L. Senjem: conception of the study, acquisition and analysis of data. Robert D. Brown, Jr.: conception of the study, acquisition and analysis of data, drafting significant portion of manuscript and figures. Michelle M. Mielke: conception of the study, acquisition and analysis of data, drafting significant portion of manuscript and figures. Rosebud O. Roberts: conception of the study, acquisition and analysis of data, drafting significant portion of manuscript and figures. Val J. Lowe: conception of the study, acquisition and analysis of data, drafting significant portion of manuscript and figures. David S. Knopman: conception of the study, acquisition and analysis of data, drafting significant portion of manuscript and figures. Ronald C. Petersen: conception of the study, acquisition and analysis of data, drafting significant portion of manuscript and figures. Walter Kremers: acquisition and analysis of data, drafting significant portion of manuscript and figures. Prashanthi Vemuri: acquisition and analysis of data. Clifford R. Jack, Jr.: conception of the study, acquisition and analysis of data, drafting significant portion of manuscript and figures. Kejal Kantarci: conception of the study, acquisition and analysis of data, drafting significant portion of manuscript and figures.


## Study funding

Research reported in this publication was supported by the National Institute on Aging of the NIH under award K76AG057015 and the NIH (AG006786, AG011378, NS097495, AG16574), and the GHR Foundation.


## Disclosure

J. Graff-Radford: funded by the National Institute on Aging of the NIH under award K76AG057015. H. Botha, A. Rabinstein, J. Gunter, S. Przybelski, T. Lesnick, J. Huston III, K. Flemming, G. Preboske, M. Senjem, and R. Brown, Jr. report no disclosures relevant to the manuscript. M. Mielke reports consulting for Lysosomal Therapeutics Inc. and Eli Lilly and Company and receiving research funding from the NIH, Biogen, and Roche. R. Roberts reports receiving research funding from the NIH, Roche, and Biogen. V. Lowe reports consulting for Bayer Schering Pharma, Merck Research, and Piramal Imaging Inc. and receives research support from GE Healthcare, Siemens Molecular Imaging, Avid Radiopharmaceuticals, the NIH (National Institute on Aging, National Cancer Institute), the Elsie and Marvin Dekelboum Family Foundation, the Liston Family Foundation, and the MN Partnership for Biotechnology and Medical Genomics. D. Knopman receives research support from the NIH and the Robert H. and Clarice Smith and Abigail Van Buren Alzheimer's Disease Research Program of the Mayo Foundation. He serves on a data safety monitoring board for Lundbeck Pharmaceuticals and for the Dominantly Inherited Alzheimer Network study and is an investigator in clinical trials sponsored by Biogen, TauRx Pharmaceuticals, Lilly Pharmaceuticals, and the Alzheimer's Disease Treatment and Research Institute, University of Southern California. R. Petersen works as a consultant for Merck Inc., Roche Inc., Biogen Inc., Eli Lilly and Company, and Genentech Inc.; receives publishing royalties for *Mild Cognitive Impairment* (Oxford University Press, 2003); and receives research support from the NIH and the Robert H. and Clarice Smith and Abigail Van Buren Alzheimer's Disease Research Program of the Mayo Foundation. W. Kremers reports receiving research funding from AstraZeneca, Biogen, and Roche. P. Vemuri receives research funding from the NIH. C. Jack, Jr. receives research funding from the NIH and the Alexander Family Alzheimer's Disease Research Professorship at Mayo Clinic, and consults for Eli Lilly and serves on the data safety monitoring board for Roche but accepts no honoraria for these services. K. Kantarci serves on the data safety monitoring board for Takeda Global Research & Development Center, Inc., and receives research support from the NIH. Go to Neurology.org/N for full disclosures.


## Publication history

Received by *Neurology* March 16, 2018. Accepted in final form September 10, 2018.


## References


1. Poels MM, Vernooij MW, Ikram MA, et al. Prevalence and risk factors of cerebral microbleeds: an update of the Rotterdam Scan Study. Stroke 2010;41:S103–S106.

2. Akoudad S, Portegies ML, Koudstaal PJ, et al. Cerebral microbleeds are associated with an increased risk of stroke: the Rotterdam Study. Circulation 2015;132:509–516.
3. Greenberg SM, Vernooij MW, Cordonnier C, et al. Cerebral microbleeds: a guide to detection and interpretation. Lancet Neurol 2009;8:165–174.
4. Park JH, Seo SW, Kim C, et al. Pathogenesis of cerebral microbleeds: in vivo imaging of amyloid and subcortical ischemic small vessel disease in 226 individuals with cognitive impairment. Ann Neurol 2013;73:584–593.
5. Johnson KA, Gregas M, Becker JA, et al. Imaging of amyloid burden and distribution in cerebral amyloid angiopathy. Ann Neurol 2007;62:229–234.
6. Vernooij MW, van der Lugt A, Ikram MA, et al. Prevalence and risk factors of cerebral microbleeds: the Rotterdam Scan Study. Neurology 2008;70:1208–1214.
7. Romero JR, Preis SR, Beiser A, et al. Risk factors, stroke prevention treatments, and prevalence of cerebral microbleeds in the Framingham Heart Study. Stroke 2014;45: 1492–1494.
8. Sveinbjornsdottir S, Sigurdsson S, Aspelund T, et al. Cerebral microbleeds in the population based AGES-Reykjavik Study: prevalence and location. J Neurol Neurosurg Psychiatry 2008;79:1002–1006.
9. Dierksen GA, Skehan ME, Khan MA, et al. Spatial relation between microbleeds and amyloid deposits in amyloid angiopathy. Ann Neurol 2010;68:545–548.
10. Gurol ME, Dierksen G, Betensky R, et al. Predicting sites of new hemorrhage with amyloid imaging in cerebral amyloid angiopathy. Neurology 2012;79:320–326.
11. Roberts RO, Geda YE, Knopman DS, et al. The Mayo Clinic Study of Aging: design and sampling, participation, baseline measures and sample characteristics. Neuroepidemiology 2008;30:58–69.
12. St Sauver JL, Grossardt BR, Yawn BP, Melton LJ III, Rocca WA. Use of a medical records linkage system to enumerate a dynamic population over time: the Rochester Epidemiology Project. Am J Epidemiol 2011;173:1059–1068.
13. Pichler M, Vemuri P, Rabinstein AA, et al. Prevalence and natural history of superficial siderosis: a population-based study. Stroke 2017;48:3210–3214.
14. Roberts RO, Knopman DS, Syrjanen JA, et al. Weighting and standardization of frequencies to determine prevalence of AD imaging biomarkers. Neurology 2017;89: 2039–2048.
15. Jack CR Jr, Bernstein MA, Fox NC, et al. The Alzheimer's Disease Neuroimaging Initiative (ADNI): MRI methods. J Magn Reson Imaging 2008;27:685–691.
16. Kantarci K, Gunter JL, Tosakulwong N, et al. Focal hemosiderin deposits and beta-amyloid load in the ADNI cohort. Alzheimers Dement 2013;9:S116–S123.
17. Vemuri P, Gunter JL, Senjem ML, et al. Alzheimer's disease diagnosis in individual subjects using structural MR images: validation studies. Neuroimage 2008;39:1186–1197.
18. Schwarz CG, Gunter JL, Ward CP, et al. The Mayo Clinic Adult Lifespan Template: better quantification across the lifespan. Alzheimers Dement 2017;13:P93–P94.
19. Avants BB, Epstein CL, Grossman M, Gee JC. Symmetric diffeomorphic image registration with cross-correlation: evaluating automated labeling of elderly and neurodegenerative brain. Med Image Anal 2008;12:26–41.
20. Jack CR Jr, Lowe VJ, Senjem ML, et al. 11C PiB and structural MRI provide complementary information in imaging of Alzheimer's disease and amnestic mild cognitive impairment. Brain 2008;131:665–680.
21. Knopman DS, Jack CR Jr, Wiste HJ, et al. Short-term clinical outcomes for stages of NIA-AA preclinical Alzheimer disease. Neurology 2012;78:1576–1582.
22. Senjem ML, Gunter JL, Shiung MM, Petersen RC, Jack CR Jr. Comparison of different methodological implementations of voxel-based morphometry in neurodegenerative disease. Neuroimage 2005;26:600–608.
23. Lowe VJ, Kemp BJ, Jack CR Jr, et al. Comparison of 18F-FDG and PiB PET in cognitive impairment. J Nucl Med 2009;50:878–886.
24. Song XW, Dong ZY, Long XY, et al. REST: a toolkit for resting-state functional magnetic resonance imaging data processing. PLoS One 2011;6:e25031.
25. Xia M, Wang J, He Y. BrainNet Viewer: a network visualization tool for human brain connectomics. PLoS ONE 2013;8:e68910.
26. Go AS, Hylek EM, Phillips KA, et al. Prevalence of diagnosed atrial fibrillation in adults: national implications for rhythm management and stroke prevention: the AnTicoagulation and Risk Factors in Atrial Fibrillation (ATRIA) Study. JAMA 2001; 285:2370–2375.
27. DeSimone CV, Graff-Radford J, El-Harasis MA, Rabinstein AA, Asirvatham SJ, Holmes DR Jr. Cerebral amyloid angiopathy and implications for atrial fibrillation management. Lancet 2017;390:9–11.
28. Graff-Radford J, Simino J, Kantarci K, et al. Neuroimaging correlates of cerebral microbleeds: The ARIC Study (Atherosclerosis Risk in Communities). 2017;48: 2964–2972.
29. Benedictus MR, Prins ND, Goos JD, Scheltens P, Barkhof F, van der Flier WM. Microbleeds, mortality, and stroke in Alzheimer disease: the MISTRAL Study. JAMA Neurol 2015;72:539–545.
30. Sperling R, Salloway S, Brooks DJ, et al. Amyloid-related imaging abnormalities in patients with Alzheimer's disease treated with bapineuzumab: a retrospective analysis. Lancet Neurol 2012;11:241–249.
31. Sperling RA, Jack CR Jr, Black SE, et al. Amyloid-related imaging abnormalities in amyloid-modifying therapeutic trials: recommendations from the Alzheimer's Association Research Roundtable Workgroup. Alzheimers Dement 2011;7:367–385.
32. Sperling RA, Rentz DM, Johnson KA, et al. The A4 study: stopping AD before symptoms begin? Sci Transl Med 2014;6:228fs213.
33. Martinez-Ramirez S, Romero JR, Shoamanesh A, et al. Diagnostic value of lobar microbleeds in individuals without intracerebral hemorrhage. Alzheimers Dement 2015;11:1480–1488.
34. Ellis RJ, Olichney JM, Thal LJ, et al. Cerebral amyloid angiopathy in the brains of patients with Alzheimer's disease: the CERAD experience, Part XV. Neurology 1996; 46:1592–1596.
35. Rosand J, Muzikansky A, Kumar A, et al. Spatial clustering of hemorrhages in probable cerebral amyloid angiopathy. Ann Neurol 2005;58:459–462.

# Cerebral microbleeds: Prevalence and relationship to amyloid burden

Jonathan Graff-Radford, Hugo Botha, Alejandro A. Rabinstein, et al.

*Neurology* published online December 19, 2018
DOI 10.1212/WNL.0000000000006780